Examination of the structural poperties of the $H_3O^+(H_2O)_n$ clusters in the (μPT) Grand Canonical ensemble, by employing a new many-body potential-energy function

Sergey V. Shevkunov
Physics and Mechanics Department, St. Petersburg State Technical University, 29 Politekhnicheskaya ul., St. Petersburg, 195251 Russia

Alice Vegiri[a)]
National Hellenic Research Foundation, Institute of Theoretical and Physical Chemistry, 48 Vas. Constantinou Av., Athens, 11 635 Greece

(Received 12 April 1999; accepted 31 August 1999)

In the current work we examine the structural properties of water clusters that result from the hydration of a rigid H_3O^+ ion, under thermal conditions at $T=250$ K and for four different vapor pressures at 0.0156, 0.0625, 0.25, and 1 mbar. For this purpose we have constructed a model potential function that accounts explicitly not only for the three-body but for all orders of many-body interactions between the ion and the water molecules and for charge transfer effects as well. The adjustable parameters of the potential have been derived within $\sim 0.1 k_B T$ accuracy through a concurrent fit to experimental enthalpy and entropy values from the corresponding cluster growth reactions. Many-body interactions have been found to comprise $\sim$10% the three-body interactions, a fact that can not be ignored. The calculations have been carried out in the Grand Canonical ensemble (μPT) where cluster sizes with a mean number of 6.69, 9.67, 29.17, and 44.37 water molecules for the four respective vapor pressures, have been generated. We have found a steady population transfer from the contact to the ion region to the second hydration shell as the vapor pressure increases. Typical equilibrium molecular configurations consist predominantly of pentagonal and hexagonal rings, that at $p=1$ mbar completely encircle the ion, forming in this way pronounced spherical cages. Radial distribution functions, polarization, and cluster density profiles have also been calculated. © *1999 American Institute of Physics.* [S0021-9606(99)51144-6]

I. INTRODUCTION

The condensation of water droplets on ions is of central importance in atmospheric chemistry. The presence of large protonated water cluster ions of the type $H_3O^+(H_2O)_{1-22}$, in the altitude region from 80 to 90 Km where the temperatures during the summer months are in the 120–140 K range,[1–3] has suggested their possible role in the formation of the noctilucent clouds (NLC) via ion induced nucleation mechanisms. Ion induced nucleation of water vapor takes place not only in the upper atmosphere, but at lower altitudes as well. The $H_3O^+(H_2O)_{1,2,3}$ clusters are the terminal species formed through a series of reactions in the *D* region of the atmosphere.

Protonated water clusters consisting of as many as 60 water molecules have been generated in the laboratory in the 135–300 K temperature range in a series of fast flow tube experiments by Castleman *et al.*[1,4]

The knowledge of the structural properties of the water molecules around the hydronium ion is important in understanding the dynamics of the proton transfer process in solutions. There is a plethora of *ab initio* studies[5–12] aiming mainly to the investigation of the structures and energetics of the lower sequence of the protonated water cluster series.

It is known that the proton cannot exist on its own but it is attached to a water molecule with a large cohesion energy of about 165 kcal/mol to form the very stable hydronium. However, *ab initio* calculations[13–16] and graphical techniques[17] in larger clusters, have shown that the excess charge can exist not only as H_3O^+ but as $H_5O_2^+$ as well, where in this case is shared by two neighboring water molecules. Although the minimum energy structures correspond to a rigid hydronium ion, $H_5O_2^+$ centered structures have been found to be close in energy. Tuckerman *et al.*[18] in their *ab initio* molecular-dynamics (MD) calculations in the bulk estimate the percentage contribution of the H_3O^+ centered configurations visited along a long MD trajectory to 60%, whereas the $H_5O_2^+$ centered ones constitute the 40%. However, not similar estimations exist for clusters.

The necessity for the simulation of larger hydrated proton clusters arose from the magic number characteristic behavior of the $H_3O^+(H_2O)_{20}$ clusters, which have been steadily observed under different experimental techniques and conditions.[19,20] Although the hypothesis[21] for the existence of an underlying hydrogen bonded pentagonal dodecahedral structure encaging a hydronium ion, and the mixed water-TMA experiments by Castleman *et al.*[19] seemed to explain such an enhanced stability, not all *ab initio* and model calculations for these systems have been able to support this view. Highly deformed dodecahedral cages have been found to be the most stable ones with the excess proton preferen-

[a)]Electronic mail: avegiri@helix.eie.gr

tially incorporated into the cage lattice,[16,17,22,23] rather than in the middle of it, according to the results of model calculations.[20,24] The origin of the enhanced stability of the dodecahedral structure has been attributed to entropic rather than to energetic reasons.[25] It was suggested[23] that it is rather due to the excess ionic positive charge that is distributed among all the H atoms and not to Coulombic interaction[20] between the hydronium unit and the lattice.

Apart from the *ab initio* calculations, several model potential functions have also been developed over the years for the study of the hydronium ion hydration effects. Their parameters have been fitted to *ab initio* data either of the H_2O–H_3O^+ interaction[26,27] or to minimum energy structures of small ionic clusters.[28–30] These potential functions are distinguished according to whether nonadditive interactions are incorporated either explicitly,[26,30] or in the form of the self-consistent calculation of the polarization energy,[26,28–30] or both.[26,30] Their differences also lie on the way the excess proton is treated, either as a rigid hydronium ion or as a free particle. Kozack *et al.* proton model,[28] Fornili *et al.*,[26] and Buffey *et al.*[27] potential functions treat the hydronium as a rigid unit, whereas those of Lobaugh *et al.*[29] and Ojamäe *et al.*[30] are built on flexible hydronium and water molecules. Proton transfer reactions have been treated in *ab initio* molecular-dynamics simulations by Tuckerman *et al.*[18] and Parrinello *et al.*[31]

Despite the apparent limiting capabilities of models based on a rigid hydronium unit to describe the $H_5O_2^+$ centered structures, their overall performance is satisfactory when high accuracy in energies and proton transfer processes are not considered. Fornili *et al.*[26] Monte Carlo (MC) calculations in the bulk predict a four-coordinated hydronium ion and correlation functions in accordance with the experimental results of Triolo *et al.*,[32] suggesting in this way that ''…in a real system, water molecules in the vicinity of a newly formed hydronium ion relax to equilibrium configurations with a time constant smaller than the hydronium lifetime… .''

Kozack and Jordan[28] with their hydronium and proton models predict structures that do not differ significantly. Also, the Hodges *et al.*[33] rigid anisotropic site potential (ASP) potential model was able to predict minimum energy structures that were very close with *ab initio* $H_5O_2^+$ centered ones. This may be due to the fact that the proton in a $H_5O_2^+$ unit, except from the monohydrate case where it is almost equally shared in the middleway distance between the two oxygens, in all other cases it is preferentially bound closer to one of the two water molecules. This trend becomes stronger as the number of the water molecules in the cluster is increased.[13]

The main objective of the current work is the examination of the structural characteristics of the hydrated hydronium ions under thermal conditions, by employing a new potential-energy function initially designed by one of the authors S.V.S. for the study of the structural properties of the OH^- hydrates.[34] The novel features of the proposed model function is the explicit inclusion of all many-body and not only of the three-body interactions, the consideration of the charge-transfer effects pertinent to the hydration of the H_3O^+ ion and the derivation of the potential function adjustable parameters through a concurrent fitting to gas-phase experimental *enthalpies* and *entropies*[35,36] of the following cluster growth reactions $H_2O+H^+(H_2O)_{n-1} \rightarrow H^+(H_2O)_n$ at $T=300$ K and for $n=1-8$. When fitting to thermodynamic data for the calibration of a particular model intermolecular potential function, although enthalpy is a widely accepted quantity, the free energy rather than enthalpy alone is the most informative term. The reason is that free energy contains in addition the entropy term which is directly related to the density of states and, therefore, to the exact shape of the potential-energy surface. The utilization of thermodynamic data alone for the modeling of molecular interactions has been a common procedure in the literature. Popular potential models for water–water interactions, for instance, have been derived this way, with their merits and shortcomings of course.

In the present case, however, the derivation of the potential parameters is based exclusively on microscopic rather than on macroscopic information, since the experimental data concerns small clusters from $n=1,8$. By reproducing in a high accuracy the incremental enthalpies and entropies of these clusters we believe that we are also describing with the same accuracy the three, four, and higher order interactions pertaining among the molecules of the first shell, which are no more than four. The accurate description of the first shell is quite a significant step toward the correct description of the entire cluster.

Despite the fact that the so far proposed model potential functions are in a better position in predicting *ab initio* structures and energies, because of the way they have been fitted, namely to *ab initio* potential energies or structures, they fail to reproduce[26,28] thermodynamic data such as the experimental enthalpies.[25,35–38] As far as we know, entropy has not been checked. Our model is a different and independent approach, aiming to the description of the thermal regime where these potentials seem to fail. Simulations are performed at $T=250$ K, close to the temperature where the experimental enthalpies and entropies have been measured. On the other hand, the performance of our potential model in predicting *ab initio* structures and energies is expected to be low. The proposed model is a first step approach to the description of the protonated water clusters. Its transferability to the description of other phase states of these clusters can be certainly improved by incorporating into the fitting process *ab initio* data as well.

Our model assumes a rigid hydronium ion and rigid water molecules. The simulations have been carried out at $T=250$ K and at four different water vapor pressures at 0.0156, 0.0625, 0.25, and 1 mbar. In this way stable ion–water clusters with a respective mean size of 6.69, 9.67, 29.17, and 44.37 water molecules, have been generated. For the cluster generation the Grand Canonical statistical ensemble (μPT) has been employed. The advantage relative to the Canonical ensemble, is that the cluster sizes are not set beforehand arbitrarily, but they are dictated by the environmental conditions, the temperature, and the water vapor pressure. The Grand Canonical ensemble provides a more realistic description of the cluster growth in a gaseous

environment, by allowing for the material contact of the cluster with the surrounding water vapor. Water molecules are inserted into, or removed from a confining spherical cavity by a Monte Carlo procedure. The contribution of the many-body effects to the cluster binding energy is quite sensitive to the variation of the particle number in the system, and therefore, their explicit inclusion into the potential model is necessary if calculations are to be performed in the Grand Canonical ensemble.

The organization of the article is the following. Section II gives a detailed description of the model potential function. Section III gives the technical details of the simulation. Section IV is devoted to the presentation and discussion of the results and Sec. V is a concluding summary.

II. INTERACTION POTENTIAL

Previous studies of nucleation of water molecules on simple ions have led to the conclusion that the most significant systematic error introduced is from the omission of the many particle contributions. *Ab initio* calculations of water clusters on Li^+, Na^+, K^+, F^-, and Cl^- ions,[39] have shown that three particle interactions of the water–ion–water type provide the most significant contribution to the many-particle interactions, which comprise ~10% of the system's energy. Four-body interactions do not contribute more than 1% to 2%. A similar theoretical (self-consistent field) SCF calculation for the $H_3O^+(H_2O)_2$ clusters, by Kochanski[6] gives a value of 8% to 9% for the percentage contribution of the three-body terms to the cluster total stabilization energy, without the authors excluding the possibility for a significant contribution of higher order forces, especially for molecules involved in the first hydration shell.

An estimation of the many body contributions to the total energy of small water clusters has been given in Refs. 40 and 41. The percentage contribution of the second-order Moller–Plessett (MP2) three-body terms to the energy of the 3-mer, 4-mer and 5-mer is 17.2%, 24.6%, and 27.4%, respectively. Four-body terms for the 4-mer, 5-mer contribute by 2.1% and 3.56%, respectively. An almost linear dependence of the two-, three-, and four-body terms on cluster size has been observed.[40]

In the present model, the hydronium ion has been modeled as a rigid slightly pyramidal structure with a central charge $Q=4.802\,981\,0^{-10}$ cgs (centimeter-gram-second) accounting for the spherical part of the ionic field and with four additional charges for the nonspherical part of it. These point sources, with magnitudes equal to $0.250\,110^{-9}$, $0.250\,110^{-9}$, $0.250\,110^{-9}$, and $-0.750\,310^{-9}$ cgs, have been distributed on the H_3O^+ ion at the (0.0, 1.0171, 0.2961), (−0.8809, −0.5086, 0.2961), (0.8809, −0.5086, 0.2961), and (0.0, 0.0, 0.098) positions in the lab Cartesian coordinate frame. All coordinates are in Å. The Rahman and Stillinger ST2[42] potential has been employed for the description of the water–water interactions.

By adopting a rigid hydronium ion, we are certainly limiting the ability of the potential in describing dynamical features that are related to the proton transfer process, or to the description on equal footing of $H_5O_2^+$-centered structures.

A. Description of the potential model function

Analytically, it consists of the following terms:

1. A term describing the pairwise additive water–water interactions, $U_{\text{pair}}^{\text{w-w}}$

In the five centered ST2[42] potential, four equal in magnitude charges of $q=1.132\,062\,10^{-10}$ cgs units are placed on the vertices of a tetrahedron. The two positive and negative charges are located at a distance of 1.0 and 0.8 Å, respectively, from the center occupied by the oxygen atom. In this model r_{OH} is equal to 1.0 Å and the tetrahedral bond angle to 109°28′.

The full potential between all pairs of water molecules is written as

$$U_{\text{pair}}^{\text{w-w}}=\sum_{i<j}\left\{4\varepsilon_0^{\text{w}}\left(\left[\frac{\sigma^{\text{w}}}{r_{ij}}\right]^{12}-\left[\frac{\sigma^{\text{w}}}{r_{ij}}\right]^{6}\right)+s^{\text{w}}(r_{ij})\sum_{k=1}^{4}\sum_{l=1}^{4}\frac{q_k q_l}{|\mathbf{r}_k^i-\mathbf{r}_l^j|}\right\}, \tag{1}$$

ε_0^{w} and σ^{w} are equal to $5.260\,510^{-15}$ erg and 3.1 Å, respectively. $s^{\text{w}}(r_{ij})$ is an r dependent screening function, introduced so as to smooth out the exaggerated heterogeneous electric field of the point charges

$$s^{\text{w}}(r)=\begin{cases}0 & 0<r<r_L\\ (r-r_L)^2(3r_U-r_L-2r)/(r_U-r_L)^3 & r_L\leqslant r\leqslant r_U\\ 1 & r_U<r<\infty\end{cases}, \tag{2}$$

with $r_L=2.016$ Å and $r_U=3.1287$ Å. $\mathbf{r}_k^i$ is the position vector of the kth point charge of the ith molecule and r_{ij} is the distance between any two Lennard-Jones (LJ) centers. The singularities in the Coulombic potential are avoided by introducing spherical hard-core potentials on each force center of the water molecule, so that for $r_{ij}<d_0=1.55$ Å and $|\mathbf{r}_k^i-\mathbf{r}_l^j|<d_q=0.1$ Å, the corresponding pair term becomes infinite.

2. A term describing the ion–water interactions, in terms of the $U_{\text{pol}}^{\text{w}}$ polarization energy of a single water molecule in the ionic field

$$u_{\text{pol}}^{\text{w}}(\mathbf{r}_0^i)=-\frac{1}{2}\alpha_w\left[\sum_k E_k(\mathbf{r}_0^i)\right]^2, \tag{3}$$

where

$$\boldsymbol{E}_k(\mathbf{r}_0^i)=\boldsymbol{E}_k^c(\mathbf{r}_0^i)+\sum_{l=1}^{4}E_{kl}^J(\mathbf{r}_0^i). \tag{4}$$

The summation is over all k ions in the system. l runs from 1,4 and denotes the point charges of the ion that correspond to the nonspherical part of the ionic field. In the present case $k=1$. $\alpha_w=1.44$ Å^3 is the experimental value of the isotropic polarizability of a single water molecule; $\mathbf{r}_0^i$ is the coordinate vector of the geometric center of the ith water molecule; $\boldsymbol{E}_k(\mathbf{r})$ represents the electric field of the kth ion, with $\boldsymbol{E}_k^c(\mathbf{r})$ and $\boldsymbol{E}_{kl}^J(\mathbf{r})$ the spherical and nonspherical parts, respectively. The spherical part of the electric field is screened by $s^{\text{w}}(R)$ (where in this case $R_L=4.41$ Å and $R_U=6.857$ Å) in all types of interactions it is involved in. To

avoid any field singularities the ionic point charges have been assigned a hard spherical core of radius $d_i^s = 0.3$ Å.

Thus, the total polarization energy of the system due to the electric field of the ion(s) is given by

$$U_{\mathrm{pol}}^{\mathrm{w}} = \sum_i u_{\mathrm{pol}}^{\mathrm{w}}(\mathbf{r}_0^i), \tag{5}$$

where the summation is over all water molecules of the cluster.

3. Lennard-Jones $U_{\mathrm{LJ}}^{\mathrm{IW}}$ and electrostatic $U_{\mathrm{coul}}^{\mathrm{IW}}$ terms between the ion and the ith water molecule.

$$U_{\mathrm{LJ}}^{\mathrm{IW}} = \sum_i 4\varepsilon_0 \left(\left[\frac{\sigma}{R_i} \right]^{12} - \left[\frac{\sigma}{R_i} \right]^{6} \right),$$
$$U_{\mathrm{coul}}^{\mathrm{IW}} = \sum_i \sum_k^5 \sum_l^4 \frac{q_k q_l^i}{|\mathbf{r}_k - \mathbf{r}_l^i|}, \tag{6}$$

R_i is the distance from the center of the ion to the oxygen atom of the ith molecule. Summation is over all the water molecules in the system. $\varepsilon_0 = 0.515\,10^{-13}$ erg and $\sigma = 2.9636$ Å. Field singularities are avoided by a spherical hard-core potential of radius $d_0^{i-w} = 1.0$ Å. q_k is the charge of the ion and q_l^i is the lth charge of the ith molecule.

4. A term, $U_{\mathrm{D}}^{\mathrm{IW}}$ for the modeling of the nonelectrostatic attractive interactions between the water molecule and the ion. For the hydronium ion, attempts to model these interactions by means of LJ potentials only, repeatedly failed, because of the difficulty in reproducing the experimental free energy. The reason is that the narrow minimum of a LJ potential gives a very small value for the entropy.

The additive component of this particular interaction is modeled with the help of a screening function

$$u_{\mathrm{D}}(R_i) = -U_0[1 - s(R_i)], \tag{7}$$

where $s(R)$ has the same functional form as in Eq. (2). In this case $R_L = 4.41$ Å and $R_U = 6.875$ Å. The final expression is summed over all water molecules in the system

$$U_{\mathrm{D}}^{\mathrm{IW}} = \sum_i u_{\mathrm{D}}(R_i). \tag{8}$$

5. A term, $\tilde{U}^{\mathrm{ww}}$ for the modeling of water–ion–water many-body exchange interactions at the close to the ion region

$$\tilde{U}^{\mathrm{ww}} = \alpha_0 \left(\sum_{i<j} (\tilde{s}(R_i)\tilde{s}(R_j) \exp(-r^{ij}/b_0))^n \right)^{1/n}, \tag{9}$$

where, α_0 is an amplitude factor, b_0 is a characteristic interaction radius, R_i is the distance from the center of the ion to the oxygen atom of the ith water molecule, and r^{ij} is the distance between the geometric centers of the ith and jth water molecules. The nonlinear parameter n accounts for the magnitude of the many-body effect. In the limiting case $n = 1$, Eq. (9) reduces to the three-body exchange interactions.

$$\tilde{s}(R) = \begin{cases} 1 & 0 < R < \tilde{R}_L \\ 1 - (R - \tilde{R}_L)^2 (3\tilde{R}_U - \tilde{R}_L - 2R)/(\tilde{R}_U - \tilde{R}_L)^3 & \tilde{R}_L \leqslant R \leqslant \tilde{R}_U \\ 0 & \tilde{R}_U < R < \infty \end{cases}, \tag{10}$$

$\tilde{R}_L = 3.932$ Å and $\tilde{R}_U = 6.669$ Å.

Expressions (9) and (10) are valid for a single ion. When more than one ions are present, then R is defined as the distance to the nearest ion.

6. A term, $U_{\mathrm{tr}}^{\mathrm{ww}}$ which describes in an explicit way the Coulombic repulsion forces between two water molecules that carry an excess electric charge. This charge is due to the fractional charge ΔQ_i that has been transferred from the ion to the neighboring ith water molecule. This results into a dipole

$$\boldsymbol{p}_i = \Delta Q_i \boldsymbol{R}_i, \tag{11}$$

where $\boldsymbol{R}_i$ is the vector directed from the ion to the ith molecule. ΔQ_i depends on the distance as follows:

$$\Delta Q_i = \kappa \cdot \tilde{s}(R_i) \cdot Q, \tag{12}$$

κ is a parameter that varies in the [0,1] range and which describes the degree of the charge-transfer process. $\tilde{s}(R)$ is given by Eq. (10).

The interaction between the transferred charges is represented in the form of interacting dipoles

$$U_{\mathrm{tr}}^{\mathrm{ww}} = \sum_{i<j} \left(\frac{(\mathbf{p}_i \cdot \mathbf{p}_j)}{\mathbf{r}_{ij}^3} - 3(1-\gamma) \cdot \frac{(\mathbf{p}_i \cdot \mathbf{r}_{ij})(\mathbf{p}_j \cdot \mathbf{r}_{ij})}{r_{ij}^5} \right). \tag{13}$$

The parameter γ is a correction associated with the finite size of the dipoles. For $\gamma = 0$ Eq. (13) reduces to the expression for the interaction energy between two point dipoles. The second term in the right-hand-side of Eq. (13) reflects the anisotropy of the interaction with respect to the $\mathbf{r}_{ij}$ vector connecting the ith and jth water molecules. γ varies in the [0,1] interval. Expression (13) is regarded as an approximate one and as a small correction to the leading terms of Eq. (9). The way that the screening functions $s(\tilde{R})$ are introduced into Eq. (9) ensures that the corresponding many-body terms in the expansion differ from zero, only after all of the water molecules that are involved into this term are found concurrently at the ion neighborhood.

The potential function describing the total interaction of a single ion with a number of water molecules is given by the summation of terms 1–6.

$$U^{\mathrm{tot}} = U_{\mathrm{pair}}^{\mathrm{w-w}} + U_{\mathrm{coul}}^{\mathrm{IW}} + U_{\mathrm{pol}}^{\mathrm{w}} + U_{\mathrm{LJ}}^{\mathrm{IW}} + U_{\mathrm{D}}^{\mathrm{IW}} + \tilde{U}^{\mathrm{ww}} + U_{\mathrm{tr}}^{ww}. \tag{14}$$

B. Derivation of the potential parameters

The experimental data on the free energy of formation of protonated water clusters[35,36] shows that the attachment of every additional water molecule to the cluster causes a change of the entropy term. This effect is more pronounced in the case of molecular ions of the type H_3O^+ and OH^-. The hydronium ion H_3O^+ is produced as a result of the dissociation of a water molecule $H_2O \leftrightarrow H^+ + OH^-$, after which

the free proton is captured with a very large cohesion energy (165 kcal/mol) by a neutral water molecule to form the hydronium ion, $H^+ + H_2O \leftrightarrow H_3O^+$. The second molecule is attached with a cohesion energy of 36 kcal/mol, the third one with an energy of 22.3 kcal/mol, the fourth with 17 kcal/mol and so on.

If a comparison is to be made with the hydration behavior of the much studied alkali halides, we note that the experimental hydration enthalpies of the H_3O^+ ion are higher than those of the halide ions[43,44] for different numbers of molecules. Despite this fact, the Na^+–Cl^- system is unstable in an aqueous solution at room temperature and disintegrates with high probability, whereas the dissociation of the H_2O molecule in liquid water is a very low probability process, $K_w = 10^{-14}$.

The explanation of the different behavior of these ions in liquid water should lie in the different structure of their hydration shells, which in turn is closely related to the entropy of hydration. The experimental entropies for a water molecule attachment to H_3O^+ (-33.3, -29, -28.3, -32.6, -30.3, -29.6, -27 cal K^{-1} mol^{-1} for $n=1-7$) tend to larger values with increasing cluster size n, whereas the entropies for the attachment of a water molecule to Cl^- (-16.5, -20.8, -23.2, -25.8 cal K^{-1} mol^{-1} for $n=1-4$) tend to lower values as n increases. This means that the hydration shell of the H_3O^+ ion is less compact than that of Cl^-, a fact that might explain their different solubility in water.

The method followed for the fitting was that of the successive approximations, where several hundreds of runs have been performed in the bi-canonical statistical ensemble by the Monte Carlo method. At every run the free energy of the corresponding ionic clusters has been calculated by the method developed in Ref. 45. The same procedure was then repeated in the canonical statistical ensemble for the calculation of the internal energy.

The comparison between the experimental and the fitted values of the internal U_N and the free energy G_N, for the $H_3O^+(H_2O)_{n=1-7}$ clusters, are displayed in Table I.

$$U_N = \sum_{n=1}^{N} \Delta U_{n-1,n} \quad \text{and} \quad G_N = \sum_{n=1}^{N} \Delta G_{n-1,n}.$$

The numerical values of the parameters of the total potential function are summarized in Table II.

Regarding the value of the nonlinear parameter n, if it were equal to one, this would mean that only three-body terms would have been significant. The present value indicates that the higher-than-three many-body terms roughly represent the 10% of the three-body interactions.

Since the proposed potential model is in fact a pseudopotential that incorporates quantum effects and depends on temperature, it is expected to perform better at thermal energies. Nevertheless, we examined its ability in reproducing *ab initio* minimum energy structures by gradually cooling the cluster down to a temperature of about 1 K. As an example we took the $H_9O_4^+$ ion, which is known to possess a global minimum with the three water molecules hydrogen bonded to the three hydrogens of the hydronium ion, with almost linear bonds. The minimum energy structure from this potential compares well with the *ab initio* results of Ojamäe *et al.*[12,30] and Lee *et al.*[10] regarding the hydrogen bond lengths, at 1.57 Å. Corresponding *ab initio* values are 1.556[12,30] and 1.54 Å.[10] All other geometrical parameters, however, disagree as, for example, the relative orientation of the three attached water molecules and the direction of the hydrogen bonds, which have been found to be quite nonlinear, at an angle of about 40 degrees off-axis.

TABLE I. Comparison of current results for internal and free energy with experiment (Refs. 35 and 36). All values are in eV.

N	$-U_N^{\exp}$	$-U_N$	$-G_N^{\exp}$	$-G_N$
1	1.536	1.536	1.085	1.085
2	2.477	2.498	1.675	1.673
3	3.188	3.207	2.044	2.041
4	3.826	3.831	2.283	2.286
5	4.364	4.348	2.452	2.451
6	4.846	4.835	2.573	2.575
7	5.267	5.292	2.669	2.671

III. TECHNICAL DETAILS OF THE CALCULATION

At $T=250$ K evaporation is significant and confinement in a finite volume is required in order for the cluster to be stabilized. In this respect a hard wall, purely reflective spherical cavity, with a radius of 8–10 Å has been employed. As it has been shown,[46] spherical cavities, because of their symmetry, do not bias the configurational shape and the properties of the confined clusters. The radius of the cavity has been chosen such as to prevent the direct contact of the cluster with the walls. The gap of about 1–3 Å that is left between the cavity walls and the water molecules is filled with gas-phase molecules. On the other hand, the volume of this gap is much less than the volume of a single particle in the vapor, so that the average number of molecules in this gas layer can be neglected with respect to the number of molecules in the entire cluster. The size of the cluster in this case can be regarded as coincident with the size of the system in the cavity.

The hydronium ion is located at the origin of the coordinate system and is oriented in such a way as to have its symmetry axis pointing along the z axis of the space fixed coordinate system, with the hydrogens pointing to the positive z direction.

In general, a number of 100–300 Million random Markov steps have been taken, each of them corresponding to the translation and the rotation of an individual water molecule

TABLE II. Numerical values of the adjustable parameters of the potential model.

$Q=4.802\,98\,10^{-10}$ cgs	$\varepsilon_0=0.515\,10^{-13}$ erg	$\alpha_0=0.841\,10^{-12}$ erg
$\varepsilon_0^{\mathrm{w}}=5.260\,5\,10^{-15}$ erg	$\sigma_0=2.9636$ Å	$b_0=26.2$ Å
$\sigma^{\mathrm{w}}=3.1$ Å	$d_0^{\mathrm{i-w}}=1.0$ Å	$n=1.117$
$r_L=2.016$ Å	$U_0=0.173\,110^{-11}$ erg	$\tilde{R}_L=3.932$ Å
$r_U=3.1287$ Å	$R_L=4.41$ Å	$\tilde{R}_U=6.669$ Å
$d_0=1.55$ Å	$R_U=6.857$ Å	$\kappa=0.095$
$d_q=0.1$ Å		$\gamma=0$
$d_l^s=0.3$ Å		

or to the insertion or removal of a single particle from the system. Each move is accepted or rejected according to the standard Metropolis algorithm. Every trial to displace a molecule is followed by five trials to insert or remove one. The acceptance probabilities of moves for displacement and rotation were in the 0.35–0.60 range, whereas corresponding probabilities for insertions and removals were about 0.005. Therefore, during a single run 500 000–1 500 000 actual changes of the cluster size have been recorded.

IV. RESULTS AND DISCUSSION

Information about the cluster structure is derived from the calculation of the following quantities:

1. O–O, O–H, H–H, hydrogen–ion, and oxygen–ion radial distribution functions.

2. Local density distribution functions on different planes (z_i) normal to the z axis, which is defined as the symmetry axis of the ion as function of the radial distance R and z_i.

3. Probability distribution functions of the angle θ between the dipole moment vector of the water molecule and the radial distance R from the ion to the oxygen atom of the molecule.

4. Probability distribution functions of φ, defined as the rotation angle of the molecule about its own symmetry axis. For $\varphi=0$ the molecular plane coincides with the plane defined by the z axis and the symmetry axis of the molecule.

The simulation is carried out at $T=250$ K and at four different vapor pressures, at $p=0.0156$, 0.062, 0.25, and 1 mbar, where thermodynamically stable clusters with a respective, mean molecular size of 6.69, 9.67, 29.17, and 44.37 water molecules have been generated.

A. Ion–water structure

Ion–oxygen $g_{IO}(R)$ and the half of the ion–hydrogen $g_{IH}(R)$ correlation function for the four different vapor pressures are displayed in Fig. 1. Table III contains the positions of the first maximum R_{max} and minimum R_{min} of the $g_{IO}(R)$ and $g_{IH}(R)$ correlation functions and the corresponding running coordination numbers, n_{IO} and n_{IH}. Radial distances are measured from the oxygen atom of the ion.

For the two lowest pressures examined, the water molecules are arranged into two well separated hydration shells. For these two pressures the most probable first shell positions are at about the same distance from the ion. As the pressure increases a gradual transfer of water population into the second shell is observed. Note the decrease of the amplitude of the first shell peak, when the pressure increases from 0.0156 to 0.0625 mbar and the subsequent rise of the second shell population. The running coordination number in the first shell and for the low-pressure region is very close to two, which corresponds to the coordination of excited configurations. At larger vapor pressures and cluster sizes molecules are entirely transferred into the second shell.

Regarding $g_{IO}(R)$, a direct comparison with first shell maximum and minimum radial positions for the Cl^+, Na^+, and K^+ spherical ions, for instance, cannot be made, since the simulations are for different cluster sizes, potential functions and temperatures. However, all of them place the first

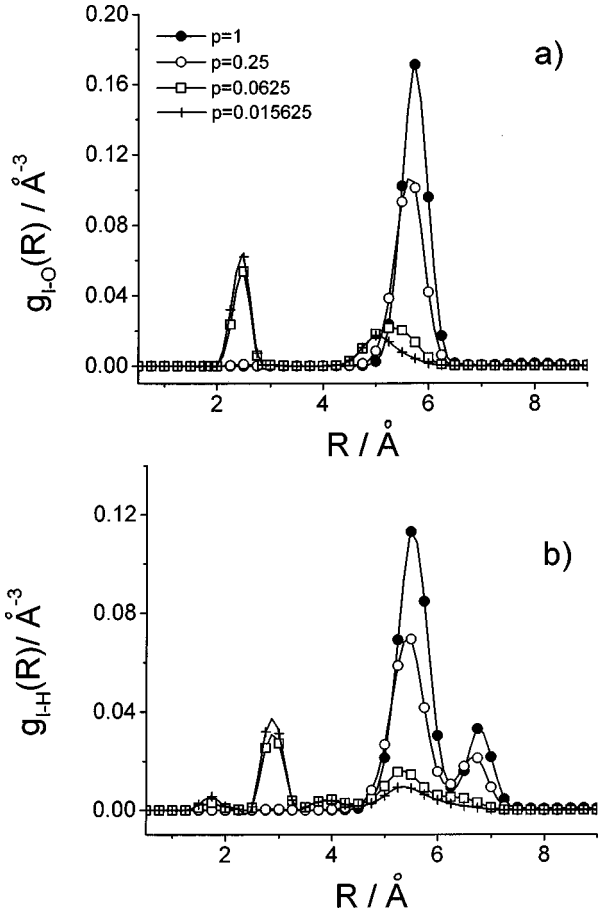

FIG. 1. (a) Ion–oxygen $g_{IO}(R)$ and (b) the half of the ion–hydrogen $g_{IH}(R)$ radial distribution function at four different vapor pressures. Pressure is in mbar.

hydration shell between 3 and 4 Å for Li^+[47] and at about 2.5 Å and 2.9 Å for Na^+[48] and K^+,[49] respectively. The most probable position of the first shell found here for the smaller hydronium water clusters is within this range of values and in particular closer to the Na^+ ion, giving thus to the hydronium an effective charge close to that of Na^+ to which it is isoelectronic. However, we believe that there are not any other similarities in contrast to Fornili *et al.*[26] speculations that the hydration properties of the hydronium and alkali metal ions are comparable.

The difference is in the strength of the hydration shell that is formed around, let us say, the Na^+ and H_3O^+ ions, by being stronger in the former case and looser in the latter. NaCl dissolves readily into water, whereas H_3O^+ recombines immediately with OH^-. Since Na^+ and H_3O^+ have similar

TABLE III. Ion–oxygen and ion–hydrogen pair correlation functions. See text for the definition of R_{max} and R_{min}. All Rs are in Å.

	$g_{IO}(R)$			$g_{IH}(R)$		
p/mbar	R_{max}	R_{min}	n_{IO}	R_{min}	R_{max}	n_{IH}
0.0156	2.45	2.86	1.95	2.85	3.38	3.82
0.0625	2.47	2.86	1.60	2.85	3.38	3.16
0.25	5.64	6.47	29.18	5.43	6.21	41.86
1.00	5.74	6.47	44.37	5.51	6.31	63.7

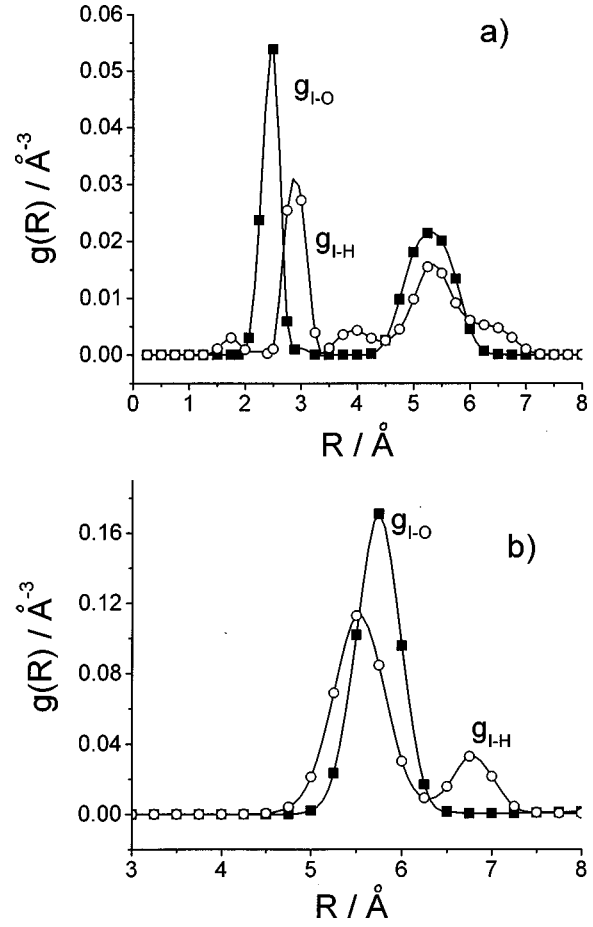

FIG. 2. Superposition of $g_{IO}(R)$ and the half $g_{IH}(R)$ radial distribution functions at (a) $p=0.0625$ mbar and (b) $p=1$ mbar.

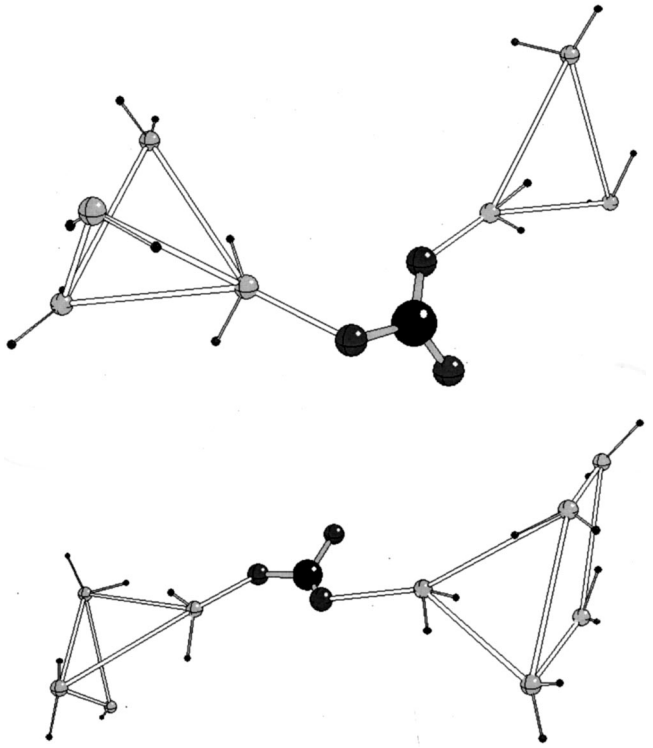

FIG. 3. Two typical equilibrium configurations for $n=7$ (upper frame) and $n=9$ (lower frame) water molecules. The black atom denotes the oxygen atom of the hydronium unit.

charges, the difference lies mainly into the degree of collectivization of the outer electrons of the ions and into their ability to transfer a portion of their excess charge. Charge-transfer processes give rise to additional repulsion forces between the ion and the water molecules and between the water molecules themselves, which partly compensate for the attractive electrostatic forces and prevent the formation of a hydration shell at close to the ion distances. Charge transfer is not significant in the alkali halide ions. For a small number of water molecules the effect of the water–water repulsion diminishes before the stronger ion–water attraction and a hydration shell close to the ion is possible to be formed.

During the fitting process we tried to find a parameter set that would reduce the charge-transfer effects by weakening the many-body interactions. In this case a stable first hydration shell at contact ion–water distances and independent of the cluster size could be obtained, but the entropy of this cluster turned out to be in large disagreement, in fact beyond any experimental uncertainty, with the experimental data of the hydration reactions. After a number of trials with various interaction models we came to the conclusion that the repulsion of the molecules from the first hydration shell in the case of the hydronium ion should be taken into consideration. This effect is completely absent in clusters described with simple pairwise additive interactions.

At this point here, we would like to compare our results with those obtained by Kelterbaum *et al.*[50] for the first 28 protonated water clusters, at $T=300$ K. The hydration scheme they propose, consisting of a tight and well-defined first shell, with position and shape independent of the cluster size, is quite different from what we find here. The procedure of the sequential filling-in of the shells would lead to significantly lower entropy values, in contradiction to experiment. On the other hand their cluster binding energies are systematically larger than the experimental values of Kebarle *et al.*

$g_{IH}(R)$ gives a qualitatively similar picture as $g_{IO}(R)$ about the population transfer to the second shell, with increasing cluster size (vapor pressure). However, at low pressures, only one significant hydrogen peak is observed in both hydration shells, indicating that both hydrogens are at the same distance from the ion and that they point away from the ion, at least in the first shell. For instance, the first significant peak of $g_{IH}(R)$ for $p=0.0625$ mbar at $R\sim 2.0$ Å lies at the right side of the first peak of $g_{IO}(R)$ at $R\sim 2.5$ Å. This is better viewed if we superimpose the $g_{IH}(R)$ and $g_{IO}(R)$ correlation functions at two indicative pressures in Fig. 2.

The fact that the value of the running coordination number for the oxygen in the first shell is almost half that of the hydrogen atom, implies that the water molecules are more likely to form a trigonal-type of bond as it has been observed for simpler cations, like Na^+,[48,51,52] Cl^+,[47] and K^+.[49]

At larger pressures, Fig. 2(b), two well-defined hydrogen peaks are observed where the first and more significant one lies slightly at the left of the oxygen peak and the second at the right. This implies that the orientational properties of the water molecules at the larger clusters are different from those at the smaller ones, and not typical of the first-shell cationic

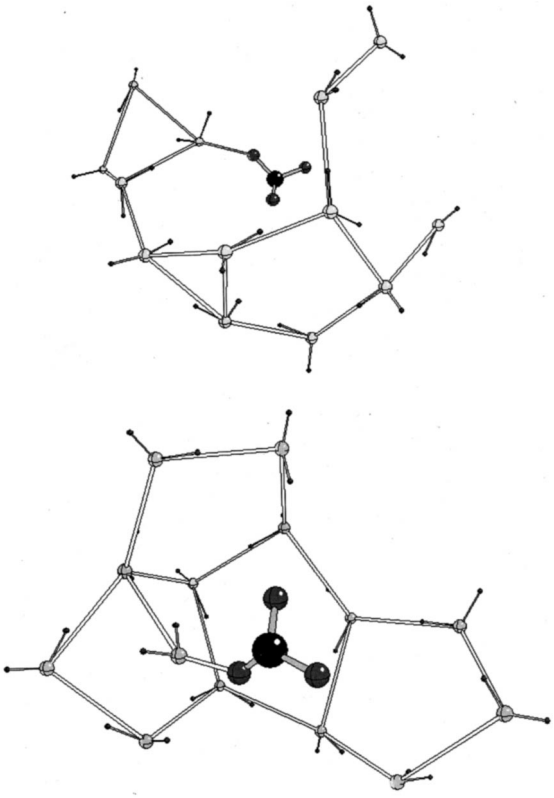

FIG. 4. As in Fig. 3 for $n=13$ (upper frame) and $n=14$ (lower frame) water molecules.

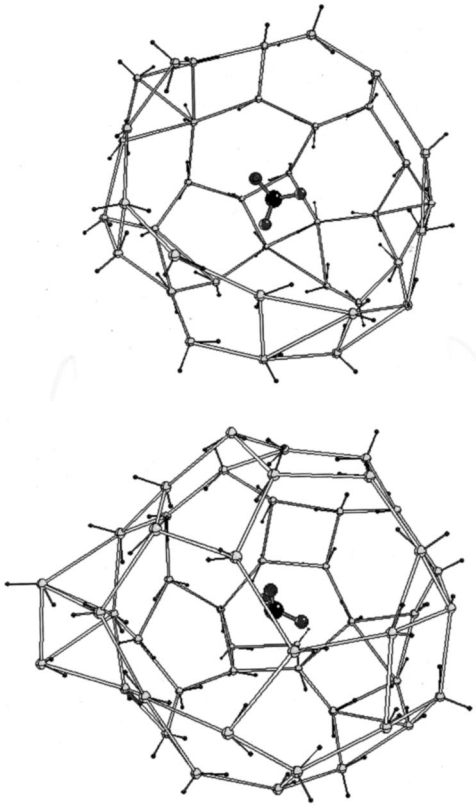

FIG. 5. As in Fig. 3 for $n=38$ (upper frame) and $n=48$ (lower frame) water molecules.

orientational preferences, where in most of the cases, only one hydrogen peak is observed. The second peak accounts for the dangling hydrogen atoms at the outer cluster surface, whose average number is equal to 16.5 for $p=0.25$ mbar and 25 for $p=1$ mbar.

A few characteristic configurations from the small, intermediate and large cluster regime are illustrated in Figs. 3–5. Figure 3 displays typical configurations with 7 and 9 water molecules. Figure 4 illustrates typical structures with 13 and 14 water molecules, whereas in Fig. 5 structures with 38 and 48 water molecules are presented. The tendency of the ion in the small clusters to be attached with two bonds to the rest of the cluster is systematically observed. As the cluster size is getting larger, the first signs for a cavity formation start to appear. At the intermediate cluster size regime $10<n<20$, before the ion gets entirely encircled, bonding is facilitated through a single bridging water molecule whereas the rest of the molecules are arranged in a manner already observed in larger structures in terms of pentagonal rings. Note that at structures with a number of molecules larger than about 10, it is not the ionic field that plays the decisive role in structuring. It is rather the hydrogen bonding between adjacent water molecules that prevails. The picture we get here is not far from the one derived from the experimental cluster binding energies.[25,38] A rapid decrease of the cohesion energy with increasing n, up to $n\sim 9$ is observed, which energy for larger clusters does not vary appreciably with size. These data place the cluster size around nine as the transition region above which the cluster stability and structure is mostly determined by the water–water hydrogen bonding interactions.

With the further rise of the cluster size, this bridging molecule is drawn into the second hydration shell, from where only sporadic visits to the ion region are observed. Clusters with a number of molecules in the 35–50 size range, tend to form deformed cages with a mean radius of about 5.5 Å, consisting mainly of pentagons and hexagons and with the ion occupying the cavity center. Bonding with several water molecules gives a lower free energy than the formation of a corresponding bond with the ion, and the water molecule prefers to be ''swallowed'' by the hydration shell, rather than to be captured by the ion. Since on the other hand, the water molecules want to form as many as possible interactions with the ion, they finally end up encircling it.

The main outcome of this work, namely the complete depletion of the first shell for cluster sizes equal and larger than about 29 molecules, seems to be in contradiction with the results of *ab initio* calculations in, let us say, the $H^+(H_2O)_{n=19-22}$, where the hydronium ion, even in the case when it is encaged it is not detached from the rest of the cluster. However, we must pay attention to the fact that the population transfer observed in our calculations happens at a temperature of 250 K. *Ab initio* calculations correspond to $T=0$ K. At the temperature of the simulation, the most probable configurations correspond not to the minimum of the potential energy, but to the minimum of the free energy, which contains the entropy term TS.

The explicit inclusion of the many-body nonadditive components in the model and the additional repulsion of neighboring water molecules because of the interaction of

the excess dipoles generated due to charge transfer from the ion, are also responsible for the cluster detachment from the ion. Usually nonadditivities are taken into account by means of induced dipole—induced dipole interactions calculated in a self-consistent way and which are responsible for these additional repulsion forces between neighboring water molecules. During the construction of the proposed potential we estimated that the inclusion of such induced polarization terms into the model would magnify the detachment tendencies.

There are several indications that the particular encaging effect is rather entropic that energetic in origin. One example is the magic number $H_3O^+(H_2O)_{20}$ clusters. The magic number does appear at $n=20$, even if the experimental binding energies[25] of these clusters from $n=6$, to $n=28$ show a smooth trend with cluster size, particularly in the $n=20$ region. It is, therefore, inferred that entropic rather energetic effects give rise to the observed magic number. Entropy becomes more significant as the number of particles increases, and as the density of states becomes larger as well. For small clusters, it is the energetic factor, through the immediate interaction of the ion with the water molecules, that decides the cluster structure, whereas for large clusters, $n>12$ structural effects come into play.

Another equally important factor that determines the solvation of an ion is the ability of a particular system to manifest significant many-body interactions a fact that is directly related to the ionic charge delocalization. F^- which is the only one from the halide ion series to form covalent bonds[43] with the water hydrogen atoms, exhibits larger three-body contributions to the total cluster stabilization energy,[53] than the Cl^- ion, for instance.

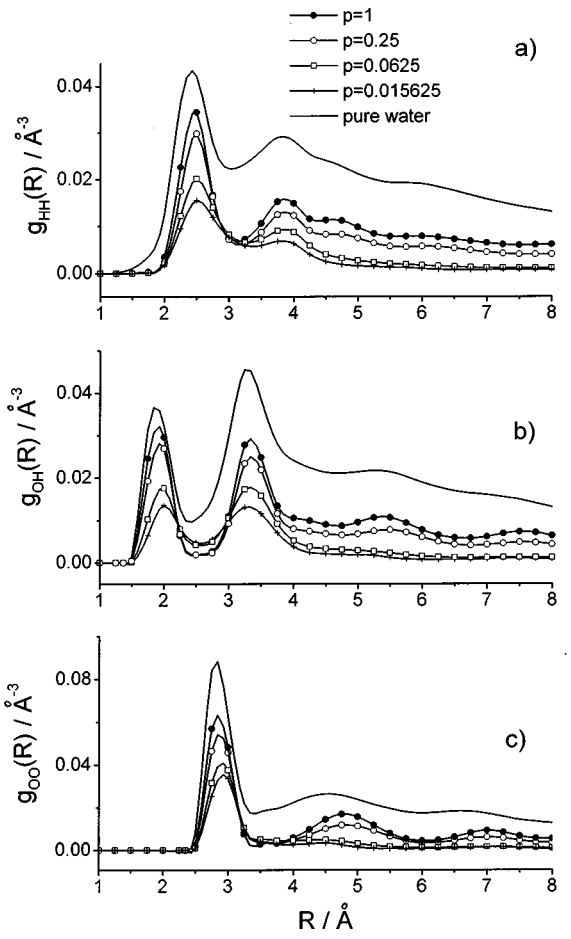

FIG. 6. H–H (a), O–H (b), and O–O (c) pair correlation functions, at four different vapor pressures. Pressure is in mbar.

B. Atom–atom pair correlation functions

Atom pair correlation functions for the four vapor pressures examined are plotted in Fig. 6. Superimposed are the correlation functions for the bulk water, which in this case is simulated as a cluster with 94 water molecules at $T=250$ K and $p=1$ mbar. For the larger clusters, three coordination shells that agree in the position of the first peak, are resolved. The secondary shells are more pronounced than in the pure water case with their positions significantly shifted to larger distances. The main features of the $g_{O-O}(R)$ pair correlation function are presented in Table IV.

Experimental values[54] for R_{max} and R_{min} for bulk water at room temperature are 2.85 and 3.32 Å, respectively. In particular, for $p=1$ mbar, the value of the oxygen coordination number indicates the existence of typical clathratelike structures which consist of triply coordinated water molecules. The experimental hydration number obtained for liquid water under the same conditions is about 4.6.

C. Orientational ordering of water dipoles

In Fig. 7 we plot the average angle between the dipole moment vector of the water molecule and the radius vector connecting the oxygen atoms of the hydronium ion and of the water molecule, as function of the radial distance from the ion, at the four vapor pressures. Positive values of $\langle \cos\theta \rangle$ correspond to dipole moment vectors that are pointing away from the ion, whereas for negative ones, the vectors are directed toward the ion. In general, we distinguish three intervals where the dipole moment vectors have alternating directions.

At short distances from the ion, (2.0–3.0 Å), which is the interval of the most probable ion–oxygen distance in the first coordination shell for the small clusters, the water molecules are oriented with their oxygens pointing to the ion, (positive $\langle \cos\theta \rangle$), where they benefit the most from the localized positive field of the hydrogen atoms of the ion. The average orientation of the water molecules changes with distance over the range of the first shell, between 54° and 90°, where the 90° orientation is assumed at the shell boundaries.

At intermediate radial distances (3–5 Å), $\langle \cos\theta \rangle$ becomes negative and the water molecules prefer to be oriented

TABLE IV. Oxygen–oxygen pair correlation function. R is in Å.

	$g_{O-O}(R)$		
p/mbar	R_{max}	R_{min}	n_{O-O}
0.0156	2.96	3.88	2.1
0.0625	2.9	3.76	2.5
0.25	2.86	3.38	2.7
1.00	2.83	3.38	3

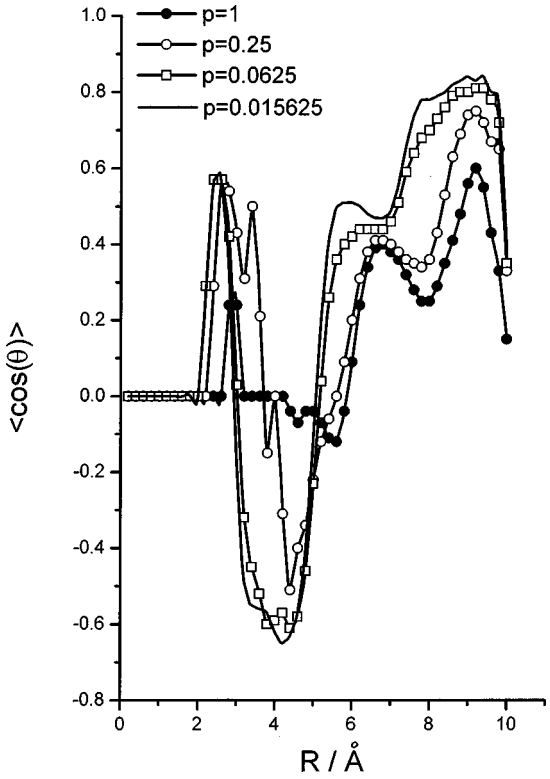

FIG. 7. Average polarization angle between the dipole moment vector of the water molecule and the radius vector pointing from the oxygen atom of H_3O^+ to the oxygen atom of the water molecule, as a function of the radial distance from the ion, at four vapor pressures. Pressure is in mbar.

with their hydrogens pointing to the ion, at a similar average orientation angle of $-54°$. As the number of molecules drawn close to the ion rises, there is an increase in the water–water and the ion–water repulsion due to the ionic charge-transfer processes. Under these conditions, the molecules prefer to be distributed around the ion rather than aggregate toward the energetically more favorable attack position of the ion, which corresponds to the side of the localized protons. This tendency is intensified at nonzero temperatures, where the entropic term in the free energy $G=U-TS+pV$ of the system becomes important and the state that corresponds to the molecules being arranged around the ion becomes that of higher entropy. In this case the optimum arrangement of several water molecules is from the side of the oxygen atom, which by displaying a more dispersed charge distribution with a consequent reduced directionality and strength of the ion–water interactions, the formation of hydrogen bonds with several neighboring water molecules is more probable. In this region water molecules turn out to be oriented with their hydrogen atoms towards the H_3O^+ ion, despite of its positive charge as a whole.

At distances, greater than about 6 Å, the spherical part of the Coulombic interactions will prevail and the water molecules will be oriented with their hydrogens pointing away from the ion. As a consequence, the orientation pattern does not change appreciably with distance. The pronounced directionality of the ion–water interaction is in principle quantum in character and it is manifested at small enough distances from the ion.

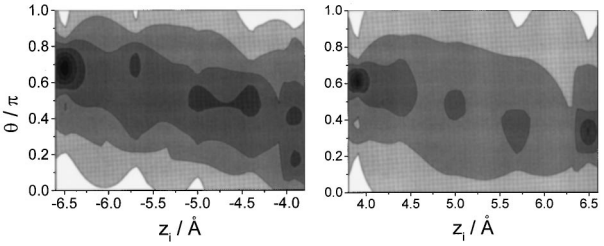

FIG. 8. Probability distribution function of the polarization angle θ at z_i plane cuts along the negative (left panel) and the positive (right panel) z axis. $p=1$ mbar.

A tendency observed in Fig. 7 is the clear decrease of the overall average polarization effect as the cluster size increases, a fact that has also been observed for the K^+ ions.[49] The impact of the ionic field anisotropy on the radial variation of the average polarization angle is indicated in Fig. 8, where the polarization angle probability distributions on x-y planes perpendicular to specific z_i cuts along the z axis are shown. These plots have been taken at $p=1$ mbar. The right panel shows the distribution at plane cuts along the positive z axis (hydrogen side of the ion), whereas the left panel shows similar cuts along the negative segment of the z axis (oxygen side of the ion). Only slabs greater than $z_i=|3.9|$ Å are displayed.

At a first sight we observe that the anisotropy of the ionic field is affecting the polarization of the water molecules according to which hemisphere of the cluster they are found. In general the polarization is stronger at the cluster poles and at the region close to the hydrogen atoms of the ion, at $z_i \sim 4.0$ Å.

At $z_i=6.5$ Å we find that the most probable angle is about 60°, which is within the range of values of the average polarization angle of the cluster at radial distances greater than 6.5 Å, see Fig. 7. The water molecules at the positive (north) cluster pole are found with their oxygens pointing to the hydrogens of the hydronium ion.

However, at $z_i=-6.5$ it turns out that the most probable angle is about 125°, which means that the water molecules are pointing toward the oxygen atom of the ion with their hydrogens. From Fig. 8, we see that the most stringent polarization forcing is observed at the region close to the hydrogen atoms of the ion, at the positive hemisphere, at $z_i=4.0$ Å. This is a consequence of the strong localization of the positive charge of the protons. Here the most probable orientational angle is $\sim 110°$, with the hydrogens pointing to the ion. This means that not only molecules found at the negative hemisphere can be polarized with their hydrogens toward the ion, but it can also happen to molecules that are found at the interior region of the positive hemisphere as well. In contrast to the strong polarization of the water molecules found closer to the hydrogen atoms of the ion, the water molecules that are found at the region close to the oxygen atom of the ion, at $z_i \sim -4.0$ Å, are loosely polarized. In fact they can orient their dipole moments in a wide range of angles with an almost equal probability. This behavior is a consequence of the diffusion of the negative charge of the ion relatively to the positive one, which is strongly localized.

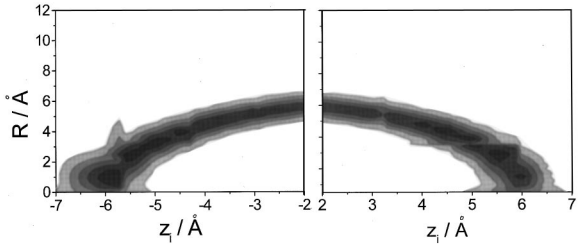

FIG. 9. Probability distribution function of the cluster density at z_i plane cuts along the negative and the positive z axis as function of the radial distance. $p=1$ mbar. Highest contour (black) is between 0.095 and 0.11 $Å^{-3}$. Contour spacing is 0.015 $Å^{-3}$.

Regarding the orientation ϕ of the water molecule plane with respect to the z axis, for $p=1$ mbar we observe that at the cluster surface, irrespective of the hemisphere, the most probable value is 0°. In the interior of the cluster, the same way as for θ, polarization is more intense for the water molecules lying at the region closer to the hydrogen atoms of the ion with most probable $\phi \sim 65°$. For the molecules closer to the ionic center from the oxygen side (negative hemisphere), ϕ polarization is less stringent, although the value of $\sim 65°$ is the most probable.

D. Density distributions

The radial density distribution as function of R and z_i along the positive and negative z axis is displayed in Fig. 9. The clusters at $p=1$ mbar and $T=250$ K are to a very good approximation spherical with a rather uniform distribution of the water molecules around the ionic center. In fact, they slightly prefer to aggregate closer to the cluster poles rather than at equatorial planes.

V. CONCLUDING REMARKS

In this work we present a new, built on thermophysical grounds, rigid many-body potential function for the description of the protonated water clusters. Apart from the many-body water–ion–water interactions, separate terms have been considered to account for the charge-transfer processes that take place from the ion to the neighboring water molecules. The potential adjustable parameters have been derived through fitting with a $\sim 0.1\ k_BT$ accuracy to experimental[35,36] incremental *enthalpy* and *entropy* values at $T=300$ K for the corresponding proton hydration reactions $H_2O+H^+(H_2O)_{n-1} \rightarrow H^+(H_2O)_n\ \ n=1-8$.

Entropy is directly related to the density of states and, therefore, to the shape of the potential-energy surface. The consideration of entropy information as well, instead of enthalpy alone, increases the reliability of the potential function. The microscopic thermodynamic information we are using, ensures the correct description of the many-body interactions at least in the first shell, which shell dictates the behavior of the cluster as a whole in a large degree.

Our model, by assuming a rigid hydronium does not take into account $H_5O_2^+$ centered configurations which in several cases are found close in energy with H_3O^+ centered ones.

We have found that the many-body water–ion–water interactions constitute about the 10% of the three-body interactions, the same way that three-body interactions comprise approximately the 10% of the corresponding two-body interaction in similar ionic or neutral water clusters.

The simulations of the protonated water clusters have been carried out in the Grand Canonical ensemble, which is more appropriate in describing cluster growth processes, in a sense that the cluster size to be studied is not arbitrarily predetermined, but it is derived in a natural way according to the external temperature and vapor pressure conditions.

The many-body water–ion–water correlations are responsible for the appearance of a long-range order which results in the generation of larger in size clusters and in the creation of cagelike structures, with a detached ion occupying the cavity center. The onset of the caging effect appears as early as from $n=10$ water molecules, where the hydronium ion, as the cluster size increases, shifts progressively from configurations where it is doubly hydrogen bonded to water molecules, to those where it is bonded to a single bridging molecule before it becomes completely encaged. The resultant structures are the result of the many-body interactions incorporated into the potential function, since trial simulations with a pairwise additive potential result into structures of the space-filling type.

Attempts to derive a potential function that would assume a sequential filling of the hydration shells, namely the second shell would be filled in only after the first one had been completed, consistently led to very small entropy values, in contradiction to the experimental results by Kebarle.

The effects of the nonspherical ionic field are visible in the orientation of the water molecules in the cluster by being strongly polarized at the region closer to the localized proton charges of the H_3O^+ ion and less polarized at the region of the dispersed oxygen charge of it. The polarization of the molecules is mainly dictated by the proton field at the close and distant from the ionic center regions. Only at intermediate distances from the ion, the orientation of the dipole moment vector is determined by the anionic field of the oxygen atom of the H_3O^+ ion.

At the larger cluster size regime, the nonspherical field is only slightly manifested in the density probability distributions. The density seems to be slightly increased in the area close to the poles rather than at the cluster equator. However, not any ''north–south'' pole asymmetry is detected. Because of the prevalence of the strong water–water correlation effects, the bridging molecules between the ion and the rest of the cluster, that have been found to exist at smaller sizes, as the size is increased they are drawn into the second hydration shell. In this way the density in the inner region of the cluster closer to the ion is significantly reduced. The majority of the water molecules lie at the cluster periphery where they have similar and not conflicting orientational preferences and this is a reason why a nearly spherical shape is achieved, as if a spherical ion has been occupying the cluster center.

ACKNOWLEDGMENTS

Financial support by NATO Grant Nos. CRG.LG-973972 and the PST.CNS-975408 is gratefully acknowledged.

[1] X. Yang and A. W. Castleman, Jr., J. Geophys. Res. **96**, 22573 (1991).
[2] R. G. Keesee, J. Geophys. Res. **94**, 14683 (1989).
[3] G. C. Reid, J. Geophys. Res. **94**, 14653 (1989).
[4] X. Yang and A. W. Castleman, Jr., J. Am. Chem. Soc. **111**, 6845 (1989).
[5] H. P. Cheng, R. N. Barnett, and U. Landman, Chem. Phys. Lett. **237**, 161 (1995).
[6] E. Kochanski, Chem. Phys. Lett. **133**, 143 (1987).
[7] A. Lami and G. Villani, J. Mol. Struct.: THEOCHEM **330**, 307 (1995).
[8] A. Lami and G. Villani, Chem. Phys. Lett. **238**, 137 (1995).
[9] Z. Latajka and S. Scheiner, J. Mol. Struct.: THEOCHEM **234**, 373 (1991).
[10] E. P. F. Lee and J. M. Dyke, Mol. Phys. **73**, 375 (1991).
[11] Y. Xie, R. B. Remington, and H. Schaefer III, J. Chem. Phys. **101**, 4878 (1994).
[12] L. Ojamäe, I. Shavitt, and S. J. Singer, Int. J. Quantum Chem., Symp. **26**, 657 (1995).
[13] D. Wei and D. R. Salahub, J. Chem. Phys. **101**, 7633 (1994).
[14] D. Wei and D. R. Salahub, J. Chem. Phys. **106**, 6086 (1997).
[15] Hai-Ping Cheng, J. Phys. Chem. A **102**, 6201 (1998).
[16] K. Laasonen and M. L. Klein, J. Phys. Chem. **98**, 10079 (1994).
[17] S. McDonald, L. Ojamäe, and S. J. Singer, J. Phys. Chem. A **102**, 2824 (1998).
[18] M. Tuckerman, L. Laasonen, and M. Sprik, J. Chem. Phys. **103**, 150 (1995).
[19] S. Wei, Z. Shi and A. W. Castleman, Jr., J. Chem. Phys. **94**, 3268 (1991).
[20] U. Nagashima, H. Shinohara, N. Nishi, and H. Tanaka, J. Chem. Phys. **84**, 209 (1986).
[21] J. L. Kassner, Jr. and D. E. Hagen, J. Chem. Phys. **64**, 1860 (1976).
[22] P. M. Holland and A. W. Castleman, Jr., J. Chem. Phys. **72**, 5984 (1980).
[23] A. Khan, Chem. Phys. Lett. **217**, 443 (1994).
[24] R. E. Kozack and P. C. Jordan, J. Chem. Phys. **99**, 2978 (1993).
[25] Z. Shi, J. V. Ford, S. Wei, and A. W. Castleman, Jr., J. Chem. Phys. **99**, 8009 (1993).
[26] S. L. Fornili, M. Migliore, and M. A. Palazzo, Chem. Phys. Lett. **125**, 419 (1986).
[27] I. P. Buffey and W. Byers Brown, Chem. Phys. Lett. **109**, 59 (1984).
[28] R. E. Kozack and P. C. Jordan, J. Chem. Phys. **96**, 3131 (1992).
[29] J. Lobaugh and G. A. Voth, J. Chem. Phys. **104**, 2056 (1996).
[30] L. Ojamäe, I. Shavitt, and S. J. Singer, J. Chem. Phys. **109**, 5547 (1998).
[31] B. L. Trout and M. Parrinello, Chem. Phys. Lett. **288**, 343 (1998).
[32] R. Triolo and A. H. Narten, J. Chem. Phys. **63**, 3624 (1975).
[33] M. P. Hodges and A. J. Stone, J. Chem. Phys. **110**, 6766 (1999).
[34] S. V. Shevkunov and D. V. Girskii, Colloid J. USSR **60**, 104 (1998).
[35] A. J. Cunningham, J. D. Payzant, and P. Kebarle, J. Am. Chem. Soc. **94**, 7627 (1972).
[36] P. Kebarle, S. K. Searles, A. Zolla, J. Scarborough, and M. Arshadi, J. Am. Chem. Soc. **89**, 6393 (1967).
[37] M. Meot-Ner and C. V. Speller, J. Phys. Chem. **90**, 6616 (1986).
[38] T. F. Magnera, D. E. David, and J. Michl, Chem. Phys. Lett. **182**, 363 (1991).
[39] H. Kistenmacher, H. Popkie, and E. Clementi, J. Chem. Phys. **61**, 799 (1974).
[40] S. S. Xantheas, J. Chem. Phys. **100**, 7523 (1994).
[41] M. P. Hodges, A. J. Stone, and S. S. Xantheas, J. Phys. Chem. A **101**, 9163 (1997).
[42] A. Rahman and F. H. Stillinger, J. Chem. Phys. **55**, 3336 (1971); F. H. Stillinger and A. Rahman, *ibid.* **57**, 1281 (1972); A. Rahman and F. H. Stillinger, J. Am. Chem. Soc. **95**, 7943 (1973); F. H. Stillinger and A. Rahman, J. Chem. Phys. **60**, 1545 (1974); **61**, 4973 (1974); A. Rahman and F. H. Stillinger, Phys. Rev. A: At. Mol, Opt. Phys. **10**, 368 (1974).
[43] M. Arshadi, R. Yamdagni, and P. Kebarle, J. Phys. Chem. **74**, 1475 (1970).
[44] I. Džidić and P. Kebarle, J. Phys. Chem. **74**, 1466 (1970).
[45] S. V. Shevkunov, A. A. Martsinovski, and P. N. Vorontsov-Velayminov, Teplofiz. Vys. Temp. (High Temperature Thermophysics) **26**, 246 (1988) (in Russian); S. V. Shevkunov, P. N. Vorontsov-Velyaminov, and A. A. Martinsinovski, Mol. Simul. **5**, 119 (1990).
[46] A. F. Terzis, P. T. Snee, and E. T. Samulski, Chem. Phys. Lett. **264**, 481 (1997).
[47] L. Perera and M. L. Berkowitz, J. Chem. Phys. **96**, 8288 (1992).
[48] R. J. Wheatley, Mol. Phys. **87**, 1083 (1996).
[49] E. N. Brodskaya and A. I. Rusanov, Mol. Phys. **71**, 567 (1990).
[50] R. Kelterbaum and E. Kochanski, J. Phys. Chem. **99**, 12493 (1995).
[51] E. Guàrdia and J. A. Padró, J. Phys. Chem. **94**, 6049 (1990).
[52] S. Zhu and G. W. Robinson, J. Chem. Phys. **97**, 4336 (1992).
[53] L. Perera and M. L. Berkowitz, J. Chem. Phys. **100**, 3085 (1994).
[54] A. K. Soper and M. G. Philips, Chem. Phys. **107**, 47 (1986).